AD-E402-343

Contractor Report ARCCD-CR-92006

TESLA COIL RESEARCH

James Corum and James Daum
Battelle
505 King Ave
Columbus, Ohio 43201-2693

Harry L. Moore
Project Engineer
ARDEC

May 1992

U. S. ARMY ARMAMENT RESEARCH, DEVELOPMENT AND ENGINEERING CENTER

Close Combat Armaments Center

Picatinny Arsenal, New Jersey

DISCLAIMER

The views, opinions, and/or findings contained in this report are those of the authors and should not be construed as an official Department of the Army position, policy, or decision, unless so designated by other documentation.

DISPOSITION INSTRUCTIONS

Destroy this report when no longer needed by any method that will prevent disclosure of contents or reconstruction of the document. Do not return to the originator.

DISCLAIMER NOTICE

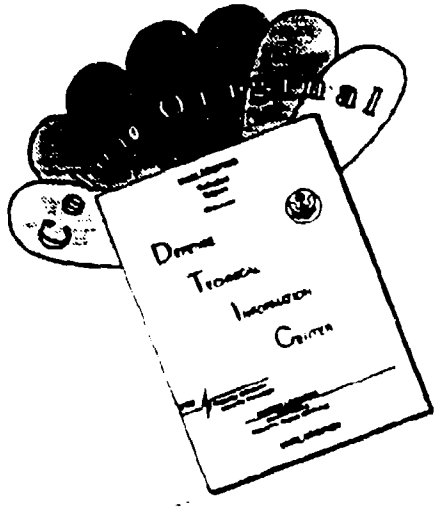

THIS DOCUMENT IS BEST QUALITY AVAILABLE. THE COPY FURNISHED TO DTIC CONTAINED A SIGNIFICANT NUMBER OF COLOR PAGES WHICH DO NOT REPRODUCE LEGIBLY ON BLACK AND WHITE MICROFICHE.

REPORT DOCUMENTATION PAGE

Form Approved
OMB No. 0704-0188

1. AGENCY USE ONLY (Leave blank)	2. REPORT DATE	3. REPORT TYPE AND DATES COVERED
	May 1992	Special/Aug 1992 - May 1992

4. TITLE AND SUBTITLE
Tesla Coil Research

5. FUNDING NUMBERS
DAAA21-90-C-0084

6. AUTHOR(S)
James Corum, Battelle
James Daum, Battelle

7. PERFORMING ORGANIZATION NAME(S) AND ADDRESS(ES)
Battelle Memorial Institute
505 King Avenue
Columbus, OH 43201-2693

8. PERFORMING ORGANIZATION REPORT NUMBER

9. SPONSORING/MONITORING AGENCY NAME(S) AND ADDRESS(ES)
ARDEC, SMCAR-CCL-FA
Picatinny Arsenal, NJ 07806-5000

10. SPONSORING/MONITORING AGENCY REPORT NUMBER
ARCCD-CR-92006

11. SUPPLEMENTARY NOTES

12a. DISTRIBUTION/AVAILABILITY STATEMENT
Approved for public release; distribution is unlimited

12b. DISTRIBUTION CODE

13. ABSTRACT *(Maximum 200 words)*

High repetition rate Tesla type high average power resonance transformers are considered in detail. Issues of RF power processing and apparatus scalability are addressed both analytically and experimentally. It has been found that, by employing appropriate switching durations and trapping energy in transmission line resonators, it is possible to increase the output of Tesla type resonance transformers by more than an order of magnitude over the conventional "k = 0.6 optimum design". The voltage step-up phenomenon is attributed to standing waves, and has been demonstrated over a frequency range that varies by more than a factor of 1,000, from VLF through VHF. While some propose using resonance transformers, because of their high average power capability, to repetitively pulse relativistic electron beams (REBs) in open air, it appears that REBs are too unstable and REB diodes are presently too fragile for practical small arms weaponry. Our investigation and experiments have led to a focused plasma discharge alternative to beams composed of fundamental particles. The technique employs a particulated macroscopic beam. This appears to be a robust directable discharge mechanism which may overcome the fragility issue for REB's. Photographic documentation and a physical explanation for the directed discharge phenomena are presented.

14. SUBJECT TERMS
RF Power, Tesla Coil, Transmission Line Resonators, Relativistic Electron Beam, Channel Seeding, Directed Discharge Ball Lightening, Electrically charged macrons

15. NUMBER OF PAGES
44

16. PRICE CODE

17. SECURITY CLASSIFICATION OF REPORT	18. SECURITY CLASSIFICATION OF THIS PAGE	19. SECURITY CLASSIFICATION OF ABSTRACT	20. LIMITATION OF ABSTRACT
unclassified	unclassified	unclassified	SAR

SUMMARY

This report summarizes an investigation into the engineering of a high voltage, high average power, compact resonance transformer device. It addresses the issue of apparatus scalability, and it documents the critical analysis and experimental verification of a new mode of operation for high power Tesla technology. In this new regime of operation, electrical energy is trapped in a slow wave helical resonator. Voltage magnification occurs during the helix's transition, from lumped element to distributed resonator, by means of the transient build-up of standing waves. The resulting voltage interference pattern has a minimum at the low impedance base and a maximum one quarter wavelength away, at the top of the helix, which is a high impedance point.

Experimental data confirms the hypothesis that the transient build-up time for wave interference on the structure is related to the spectral width of the resonator in the same manner that coherence time and spectral width are related for partially coherent optical fields. Experimental evidence also indicates that operating in such a mode permitted the attainment of RF voltages an order of magnitude greater than could be obtained by means of the so called "optimum coupled" ($k = 0.6$) Tesla coil.

Finally, experimental documentation has been given for seeded channel focused discharges in excess of eight meters in open air. Although we did not achieve the ambitious goals which we had set out for ourselves, we were able to resolve several key issues and document phenomena which were previously unpublished.

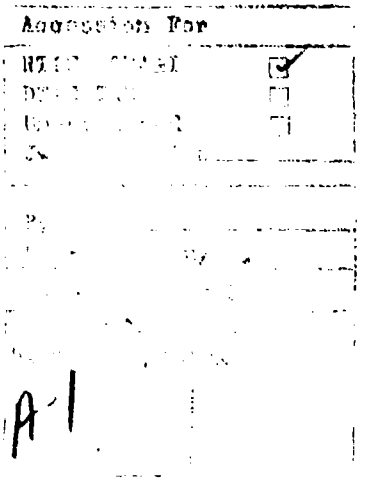

CONTENTS

FIGURES

PHOTOGRAPHS

INTRODUCTION

Objectives

This project was intended to provide scientific study and experimentation directed toward the development of an unconventional power processing technology applicable to small arms. The specific goal of the research program was to investigate the appropriateness of Tesla type resonance transformer technology for weapons power processing. This involved concept formulation, theoretical design, engineering experimentation, laboratory demonstration and testing.

Capabilities

The resonance transformer technology offers the capability not only of high voltages (in the megavolt range) with high peak powers, but also power processing with high average power levels. The latter might be appropriate for driving relativistic electron beams in a mode where they repetitively pulse a channel through the air, i.e., holeboring.

Concept

The following is a conceptual description of the apparatus studied. For the laboratory demonstration, the process was conceived to start with a 100 amp, 250 volt, primary circuit. This energy is then transformed to generate 0.70 amps at 35 kilovolts (RMS). The secondary circuit has a rotary spark gap which operates at 120 pulses/sec (but could be increased by two orders of magnitude if desired). The primary LC tank circuit operates at 100 to 150 kHz, which is inductively coupled to the secondary RF resonator. The secondary resonator comprises a resonant quarter wave, high voltage RF transformer. The resonant transformer then steps the RF voltage level up, by standing waves, to 1-5 megavolts (continuously adjustable). The resonator employed is capacitively top-loaded. The transient response-time and its relation to resonator losses and voltage rise is studied both theoretically and experimentally.

Issues to be resolved

The ultimate success of an RF powered weapon of interest to small arms hinges upon the resolution of several key issues. Can the apparatus and phenomenon be sealed electrically and physically? Is the process sufficiently stable and controllable?

Research Program

The program of research intended to resolve these issues, both analytically and experimentally, is presented in the sections below. These document our technical approach and activities in the following areas: Apparatus, Tests, Experiments and Findings, and Conclusions.

ANALYSIS AND DESIGN OF TESLA TYPE RESONANCE TRANSFORMERS

Objectives

The objective of this section is to provide an engineering analysis of the electrical apparatus used to generate the high voltages. Its purpose is to provide an analytical model sufficiently accurate to numerically predict and evaluate performance (that subsequently has been measured in the laboratory).

Since the goal of the research was a laboratory demonstration of the proposed technology, we placed considerable emphasis on the apparatus to be developed. A major issue to be resolved was whether the apparatus could be scaled down in size. As will be seen, the results of the analytical model developed below and the subsequent laboratory measurements have provided an affirmative answer to this issue.

Summary of Achievements

We have found that the published engineering literature on resonance transformer design, which is fairly extensive, is inadequate. A closer look at the physical principles has been required in order to explain phenomena which were documented as part of our research. Outside of our work in this area, there does not appear to exist an acceptable engineering analysis of resonance transformers. Consequently, we review these principles in considerable detail in this section. Further, our laboratory documentation has demonstrated that tuning for maximum VSWR (Voltage Standing Wave Ratio) can raise the energy of these devices by more than an order of magnitude over what is obtainable by the long-pulse lumped circuit operation so common in the North American and Western European accelerator community. In order to understand why and how this is possible, an analysis of the apparatus in both the lumped element (conventional) regime of operation and in the distributed regime of operation must be performed. We place critical importance on voltage rise by standing wave VSWR when engineering such structures. In particular, it was demonstrated that *lumped circuit analysis* (which is entirely appropriate *during* the energized primary regime) *totally fails* to describe *true* resonance transformers during the distributed regime. This important aspect of high voltage technology has been overlooked by previous investigators, including the Soviets in their open literature.

Specifically, we have found that it is possible to increase the output voltage of existing machines, now operating in the lumped regime, by more than an order of magnitude (provided that system breakdown does not initiate prior to attaining the peak voltage). With the new approach, it is imperative that adequate construction measures be taken to prevent electrical breakdown. The scalability issue, as will be seen below, was favorably resolved.

Engineering Analysis

The heart of the apparatus used in this project is what is commonly called a "*Resonance Transformer.*" The term was first used in an accelerator context by David Sloan, at Berkeley in the 1930's, to describe a distributed (RF transmission line) resonator.[1,2] (By the way, Sloan published

the astonishing remark that resonance transformers "cannot be treated usefully by mathematics"!) It fascinating to note that Sloan's work was actually predated by the earlier work of Nikola Tesla. Sloan *mistakenly* identified "Tesla Coils" as *lumped* tuned resonators. The *distributed resonance transformers* used by Sloan were actually patented by Tesla in the mid-1890's. This distinction has, apparently, gone unnoticed by Western researchers. Recently, Tesla's approach to high power RF power processing has enjoyed renewed interest, particularly in Russian laboratories. During 1990, Tesla transformer technology was identified by a contingent of US pulse power scientists as an "area of Soviet excellence and exceptional capability."[3,4]

The advantage of these rugged structures is that they can not only provide high peak powers (as could be done, for example, with a common Marx generator), but they can do so with high average power (high repetition rates). The Tesla resonators produce not only high voltage, but do so with high average power. From a power engineer's perspective, Van de Graaff machines, although of comparable energy, have trifling power performance. (Their power performance is limited by the mechanical power in the belt.) Although many accelerator schemes produce higher *energies* than Tesla resonators, few actually produce higher *voltages*. How does a resonance transformer generator work, and how can one get increased performance from these machines?

Analysis of Lumped Lossy Coupled Coils

We start with the transient analysis of conventional lumped, lossy, coupled, tuned circuits as shown in Figure 1.[5] We have treated the lossy case extensively in several publications.[6,7] It will be seen that this analysis is appropriate during the time that the primary spark is conducting, and we will need this information to understand how our apparatus works and how to tune it properly. The circuit shown in Figure 1 is deceptively simple! Assuming that C_1 has been charged to its peak voltage V_o, we start our analysis the moment that the gap arcs. We write the (lumped element) Kirchoff voltage laws:

$$L_1 \frac{di_1}{dt} + R_1 i_1 + \frac{1}{C_1} \int i_1 dt - M \frac{di_2}{dt} = V_o \qquad (1)$$

$$- M \frac{di_1}{dt} + L_2 \frac{di_2}{dt} + R_2 i_2 + \frac{1}{C_2} \int i_2 dt = 0 \qquad (2)$$

The mutual inductance, M, expresses the fact that the coils are "bathed" in each other's magnetic fields. Uncoupling these two linear equations will give a single fourth order differential equation for either $i_1(t)$ or $i_2(t)$. (It is simpler to solve a single variable fourth order differential equation than two simultaneous second order differential equations.) Let us start by considering the current in the secondary circuit first.

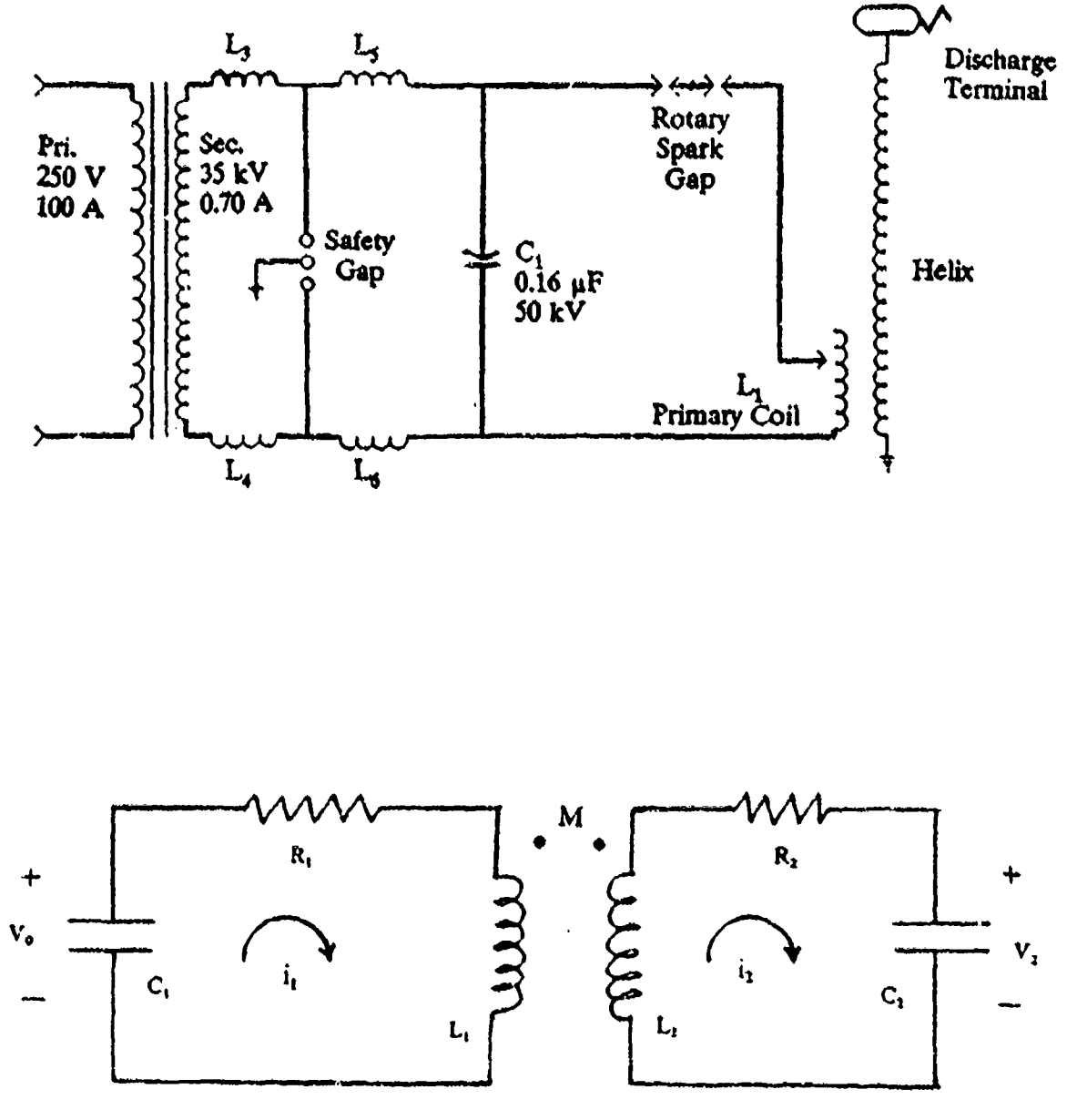

Figure 1. Equivalent circuit for the resonance transformer during the primary spark interval

The Secondary Current. When we uncouple the two integro-differential equations, we obtain the simple fourth order differential equation:

$$C_1C_2(L_1L_2-M^2)\frac{d^4i_2}{dt^4} + C_1C_2(R_1L_2 + R_2L_2)\frac{d^3i_2}{dt^3}$$
$$+ (C_1L_1 + C_2L_2 + R_1R_2C_1C_2)\frac{d^2i_2}{dt^2} + (R_1C_1 + R_2C_2)\frac{di_2}{dt} + i_2 = 0 \quad (3)$$

If we could solve this for $i_2(t)$, subject to the initial conditions, we could readily determine the voltage across the output capacitance. There is a similar fourth order differential equation for $i_1(t)$. It is exactly the same, with i_2 replaced by i_1 in the above Equation 3. (This does not mean that i_1 and i_2 are the same waveform because the initial conditions are different for the two currents.) Deriving the expressions for the initial conditions gives:

$$i_1(0) = i_2(0) = 0 \quad (4)$$

$$\left.\frac{di_1}{dt}\right|_{t=0} = -\frac{L_2V_o}{L_1L_2-M^2} \quad (5)$$

$$\left.\frac{di_2}{dt}\right|_{t=0} = -\frac{MV_o}{L_1L_2-M^2} \quad (6)$$

$$\left.\frac{d^2i_1}{dt^2}\right|_{t=0} = \frac{(R_2L_1 + R_1L_2)L_2V_o}{(L_1L_2-M^2)^2} - \frac{R_2V_o}{L_1L_2-M^2} \quad (7)$$

$$\left.\frac{d^2i_2}{dt^2}\right|_{t=0} = \frac{(R_2L_1 + R_1L_2)MV_o}{(L_1L_2-M^2)^2} \quad (8)$$

$$\left.\frac{d^3 i_1}{dt^3}\right|_{t=0} = \frac{M}{L_1}\left[\frac{d^3 i_2}{dt^3}\right] - \frac{R_1}{L_1}\left[\frac{(R_2 L_1 + R_1 L_2) L_2 V_o}{(L_1 L_2 - M^2)^2} - \frac{R_2 V_o}{L_1 L_2 - M^2}\right] + \frac{1}{L_1 C_1}\left[\frac{L_2 V_o}{L_1 L_2 - M^2}\right] \tag{9}$$

$$\left.\frac{d^3 i_2}{dt^3}\right|_{t=0} = M V_o \left[\frac{\left(\frac{L_2}{C_1} + \frac{L_1}{C_2}\right) + R_1 R_2}{(L_1 L_2 - M^2)^2} - \frac{(R_1 L_2 + R_2 L_1)^2}{(L_1 L_2 - M^2)^3}\right] \tag{10}$$

These are valid whether the resistive losses are excessive or not. However, with the resonance transformer employed in this project, we are interested in the underdamped, or oscillatory, case. The solution will be low loss, giving damped oscillations. The solutions of Equation 3, for the primary and secondary currents, are of the form:

$$i_1(t) = K_1 e^{-\alpha_1 t} \sin(\omega_1 t + \phi_1) + K_2 e^{-\alpha_2 t} \sin(\omega_2 t + \phi_2) \tag{11}$$

$$i_2(t) = K_3 e^{-\alpha_1 t} \sin(\omega_1 t + \psi_1) + K_4 e^{-\alpha_2 t} \sin(\omega_2 t + \psi_2) \tag{12}$$

The constants K_1 and K_2 are given by

$$K_{1,2} = \left[\frac{(\alpha_1^2 + \omega_1^2)(\alpha_2^2 + \omega_2^2) C_1 V_o}{\omega_{1,2}}\right] \times \tag{13}$$

$$\left[\frac{[L_2 C_2(\alpha_{1,2}^2 - \omega_{1,2}^2) - R_2 C_2 \alpha_{1,2} + 1]^2 + \omega_{1,2}^2 C_2^2 (R_2 - 2\alpha_{1,2} L_2)^2}{[(\alpha_2 - \alpha_1)^2 + (\omega_2 - \omega_1)^2][(\alpha_2 - \alpha_1)^2 + (\omega_2 + \omega_1)^2]}\right]^2 \tag{14}$$

where the subscripts before the comma are used for K_1 and those after the comma are used for K_2. The constants K_3 and K_4 are given by the expressions

$$K_{3,4} = \frac{E\,(\alpha_{1,2}^2 + \omega_{1,2}^2)^2\,(\alpha_{2,1}^2 + \omega_{2,1}^2)}{\omega_{1,2}} \tag{15}$$

and E is given by

$$E = \frac{-MC_1C_2V_0}{\sqrt{[(\alpha_2 - \alpha_1)^2 + (\omega_2 - \omega_1)^2]\;\;[(\alpha_2 - \alpha_1)^2 + (\omega_2 + \omega_1)^2]}} \tag{16}$$

The phases are given by

$$\phi_{1,2} = \tan^{-1}\left[\frac{\omega_{1,2}C_2(R_2 - 2\alpha_{1,2}L_2)}{1 - \alpha_{1,2}R_2C_2 + L_2C_2(\alpha_{1,2}^2 - \omega_{1,2}^2)}\right] - \tan^{-1}\left[\frac{(\omega_1 - \omega_2)}{(\alpha_2 - \alpha_1)}\right] \mp \tan^{-1}\left[\frac{(\omega_1 + \omega_2)}{(\alpha_2 - \alpha_1)}\right] \tag{17}$$

and

$$\phi_{1,2} = -2\tan^{-1}\left(\frac{\omega_{1,2}}{\alpha_{1,2}}\right) - \tan^{-1}\left(\frac{\omega_1 - \omega_2}{\alpha_2 - \alpha_1}\right) \mp \tan^{-1}\left(\frac{\omega_1 + \omega_2}{\alpha_2 - \alpha_1}\right) \tag{18}$$

We now need to know the values of the attenuation constants and transient oscillation frequencies. These can be obtained by Laplace transforming Equation 3 to give the secular equation

$$S^4 + AS^3 + BS^2 + CS + D = 0 \tag{19}$$

where the constant coefficients are defined as

$$A = \frac{R_1L_2 + R_2L_1}{\Delta} \tag{20}$$

$$B = \frac{\frac{L_1}{C_2} + \frac{L_2}{C_1} + R_1R_2}{\Delta} \tag{21}$$

$$C = \frac{\frac{R_1}{C_2} + \frac{R_2}{C_1}}{\Delta} \tag{22}$$

$$D = \frac{1}{C_1C_2\Delta} \tag{23}$$

$$\Delta = (L_1L_2 - M^2) \tag{24}$$

With magnetically coupled coils, a parameter called "the coefficient of coupling" is defined as $k = M/\sqrt{(L_1L_2)}$.

For lumped coupled coils, a solution of Equation 19 yields the four complex frequencies

$$s_{1,2} = -\alpha_1 \pm j\omega_1 \tag{25}$$

$$S_{3,4} = -\alpha_2 \pm j\omega_2 \tag{26}$$

The above results are particularly useful since all have been gotten in terms of circuit element values which can be readily measured in the laboratory.

The Lumped Element Regime Output Voltage. We desire $v_{C2}(t)$, the lumped element coupled tuned circuit voltage across C_2. (One should note that C_2 is not a simple physical structure if the distributed capacity of the secondary is appreciable.) This can be found by performing the following integration:

$$v_{c_2}(t) = (1/C_2) \int i_2(t)\, dt. \tag{27}$$

The resultant expression for the voltage across the *lumped* capacitance may be arranged into the convenient form:

$$V_{c_2}(t) = F_1 e^{-\alpha_1 t} \cos(\omega_1 t + \gamma_1) + F_2 e^{-\alpha_2 t} \cos(\omega_2 t + \gamma_2) \tag{28}$$

where we have introduced the constants

$$F_{1,2} = \frac{-K_{1,2}}{C_2 \sqrt{\alpha_{1,2}^2 + \omega_{1,2}^2}} \tag{29}$$

$$\gamma_{1,2} = \Psi_{1,2} + \theta_{1,2} \tag{30}$$

$$\theta_{1,2} = \tan^{-1}\left(\frac{-\alpha_{1,2}}{\omega_{1,2}}\right) \tag{31}$$

and the quantities $K_{1,2}$, $\alpha_{1,2}$, $\omega_{1,2}$, and $\Psi_{1,2}$ are all functions of the circuit parameters as defined above.

Finally, we observe that the equations for the currents may be placed in an envelope-and-phase form which is of considerable value. For example,

$$i_2(t) = R(t)\cos[\omega_1 t + \zeta(t)] \tag{32}$$

The phase $\zeta(t)$ is a function of the spectral spread $\Delta\omega$, where

$$\Delta\omega = \omega_2 - \omega_1 \tag{33}$$

The envelope is expressed by

$$R(t) = \sqrt{K_3^2 e^{-2\alpha_1 t} + K_4^2 e^{-2\alpha_2 t} + 2K_3K_4 e^{-(\alpha_1 + \alpha_2)t}\cos(\Delta\omega t + \psi_1 - \psi_2)} \tag{34}$$

This last expression is extremely useful. When it is at its peak, the maximum energy is present in the secondary. It is at this instant that we desire the primary spark to break, making the primary mesh an open circuit (an infinite impedance). Such performance by the primary switch would "trap" all the electromagnetic energy so that it could only collapse into the secondary.

Spark Durations. As an example of the value of the expression for R(t), we can now find the instant when $i_2(t)$ is a maximum. We designate this instant as the desired spark *dwell* t_s. This gives a rather complicated equation to solve for t_s. However, the problem is simplified if we consider the relatively low loss case where the exponentials are slowly decaying. [This is a classical adiabatic invariant.] In this situation, taking the derivative, setting it equal to zero and solving for t_s gives the instant of envelope maximum as

$$t_s = \frac{\psi_2 - \psi_1}{\Delta\omega} \tag{35}$$

The effect of including losses will reduce the actual value of t_s somewhat. (It is always better to actually calculate R(t) and read off t_s than to use the low loss rule of thumb.) For a low loss circuit $\psi_1 = 0$ and $\psi_2 = \pi$. Thus, for low losses, the instant at which the envelope of $i_2(t)$ is maximum is approximately $t_s = 1/(2\Delta f)$. This is half the "beat period" of the envelope of $i_2(t)$. Since $\Delta f = kf_0$, the tighter the coupling, the greater the spectral spread *and the smaller the spark duration must be made.* The rate of transfer of energy from the primary to the secondary depends upon the tightness of coupling. For high power machines, tight coupling (large mutual inductance) is desired. This, in turn, requires very short spark durations. If long spark durations must be employed loose coupling (on the order of k_c) is desirable. The problem with such operation, however, is less than optimum output.

The envelope of $i_2(t)$ is maximum at the same instant that the envelope of $i_1(t)$ passes through zero. At this instant, all of the energy initially stored in C_p has been transferred to the secondary. Physically, t_s is how long we want the spark to last in the primary - and no longer - for the energy exchange in the coupled oscillator to go through to completion. Being able to control the spark depends upon the construction of the rotary break. Rotary breaks quench the spark because

the toothed wheel or spikes move and draw out the spark until it extinguishes. The ions which are formed between the points quickly recombine to form an insulator. If extremely tight coupling is used, the gap may refuse to quench because the duration of the low current notch in R(t) may be too short to permit sufficient ion recombination in the gap to lower the conductivity. It would be desirable to have an electronic switch that would permit control of t_s, have a reverse breakdown in excess of 100 kV and be able to repetitively switch kiloampere pulses at speeds up to 500,000 per second. Is such a solid state technology available today?

In spite of intensive Soviet efforts at the Ioffe Applied Physics Institute in Leningrad, recent Russian publications indicate that appropriate high voltage solid state technology has not yet developed to the same level of performance as mechanical spark gaps, which can be made to push the limit of capacitor technology.[8 9 10] Present transistor "state-of-the-art" apparently is still not competitive with mechanical breaks. For this, and reasons of economy, we employed the classic rotary spark gap on this project.

In the analysis above we have, of course, neglected the effect of the break speed and only analyzed a single discharge of the primary capacitance. This would be acceptable provided the break speed were slow enough so that the RF oscillations ring and die during the break period.

Pulse Interval (Break Speeds). From the considerations above, we can now predict the optimum spark duration. We now ask, "What is the best break speed to run?" In the case of a single RLC tuned circuit, it is a straightforward exercise to show that the desirable PRF would be equal to the resonant frequency. The power developed, or energy flow through the machine, is related to the break speed by

$$P = \frac{1}{2} N C_1 V_0^2 \quad \textit{watts} \tag{36}$$

where N is the number of capacitive charges the source provides to C_1 per second. What limits the power delivered now is the KVA rating of the power transformer or prime power generator. Tradeoffs have to be made between the generator's ratings, the desired spark duration and pulse repetition frequency.

The theory presented above provides a very compact analysis in closed form. No numerical approximations have been used in the expressions for $i_1(t)$, $i_2(t)$, or $V_{C2}(t)$. These expressions are exact in the oscillatory case. Before turning our attention to the situation where the distributed nature of the resonator becomes important, we have one last consideration to establish.

The Lumped Element Regime Secondary Induced Voltage. In the circuit equivalent model for coupled coils, the voltage induced into the secondary follows as

$$v_{ind}(t) = M \frac{di_1}{dt} \tag{37}$$

(Notice that this is not the voltage across some "equivalent" lumped element C_2, which was derived above.) Carrying out the differentiation leads to the expression

$$v_{ind}(t) = MK_1 e^{-\alpha_1 t}[\omega_1 \cos(\omega_1 t + \phi_1) - \alpha_1 \sin(\omega_1 t + \phi_1)] \quad (38)$$
$$+ MK_2 e^{-\alpha_2 t}[\omega_2 \cos(\omega_2 t + \phi_2) - \alpha_2 \sin(\omega_2 t + \phi_2)]$$

This is the voltage induced directly into the distributed secondary, and it is a maximum at $t = t_s$, i.e. - when the envelope of $i_1(t)$ is zero. This is the instant when $i_2(t)$ is maximum.

During the spark dwell time ($t < t_s$) the RF portion of the system may be modeled by lumped coupled circuits. This is because during the primary spark, the primary and secondary are mutually "bathed" in each other's "instantaneous" external magnetic fields over their entire physical dimensions. The phase delay *between* the coils is negligible, and they behave as lumped elements for which the classical analysis of coupled coils is appropriate. (The structures are electrically small, their physical dimensions being much, much less than an appreciable portion of a free space wavelength.)

The energy interplays between the primary and secondary, building up to a maximum secondary current at t_s. In this temporal regime, it is perfectly appropriate to determine the currents $i_1(t)$, $i_2(t)$ and voltage $v_{ind}(t)$ from the lumped circuit model. Terman has observed that,

> "The secondary current is exactly the same current that would flow if the induced voltage were applied in series with the secondary and if the primary were absent."[11]

This equivalence has been extended to the case of distributed lines and resonators by R.W.P. King in a series of classic papers in which he proved that the voltage induced in a distributed transmission line by a lumped primary oscillator can be accurately represented as a point generator, located along the resonator at the center of symmetry of the primary.[12] [13] For a "monopole" resonator above a groundplane, as used in our apparatus, this equivalent point source is located at the base of the secondary.

After the primary spark extinguishes, the secondary slow wave resonator stands alone. The phase delay of current propagation *along* the helix is substantial.[14] The ***TRAPPED ENERGY*** collapses into the resonator and establishes the buildup of a slow wave VSWR pattern, which then rings down and dies out exponentially due to the resonator losses (if there is no discharge, of course).

Today, a similar phenomenon is observed in UWB (Ultra-Wideband) impulse radar. When a target (a long cylindrical structure, for example) is illuminated by a short duration pulse, the radar return consists of two components - an "early time" response term and a "late time" (or sum of exponentials) term.[15] The first corresponds to the response of the target while the RF excitation pulse (of finite duration and spatial extent) is sweeping over the target and is "forcing" a response from the "distributed circuit." During this time-interval surface excited traveling waves are shedding radiation as they propagate (i.e., the structure is behaving like a traveling wave antenna),

and standing waves are also beginning to form. The structure then starts to radiate energy like a resonant dipole antenna. After the "short pulse" has passed by, the target structure, upon which standing waves have been established, rings down at its own characteristic frequencies. We now turn to an analysis of the resonator itself.

The Helical Resonator

Perhaps the most satisfactory description of voltage rise on a helical resonator, from an engineering perspective, is that given in the references.[16 17 18 19] The analysis points out that the secondary of a Tesla transformer is, in fact, a quarter wave helical resonator with a high VSWR. (Unlike almost everything else in RF engineering, the higher the VSWR on a resonance transformer the better.) In the sinusoidal steady state, the Vmax at the top of the resonator is simply the product of the VSWR and the voltage injected into the base of the resonator (the place of the Vmin). To the best of our knowledge, there exists no exact solution for the transient fields of a helically wound slow wave resonator. (The transient response of uniform electrical resonators, such as aircraft, is currently an area of prominent research activity, but no structures with slow wave surfaces have been analyzed in the open literature that we know of.) Because resonance transformers have such high Q (narrow bandwidth), the steady state, quasi-monochromatic analysis given below is justified and proves itself to be extremely accurate for engineering purposes.

Voltage Magnification By Standing Waves. The voltage "magnification" process is most easily understood by considering the voltage rise on a generic transmission line, as shown in Figure 2.

As usual, the coordinate origin is taken at the load and (for pedagogical reasons) a time harmonic generator is assumed to drive the input end at $z = -\ell$. (We know that the spark switched sources employed are not truly monochromatic, but the sinusoidal approximation is appropriate for adiabatic resonator oscillations.) The voltage at any point along the line is a solution of the wave equation, and is given by the expression

$$V(z) = V_+ e^{-\gamma z} + V_- e^{+\gamma z} \tag{39}$$

where $z = 0$ at the load and $z = -\ell$ at the generator end. Physically, Equation 39 expresses the fact that the voltage at any point along the transmission line is the superposition of a forward travelling wave and a backward travelling wave. The resultant analytical expression describes a spatially distributed interference pattern called a standing wave. As usual, γ is the complex propagation constant $\gamma = \alpha + j\beta$. The complex constants V_+ and V_- follow from the second order partial differential equation of which Equation 39 is a solution (the "transmission line equation"), and depend upon the boundary conditions (the generator and the load).

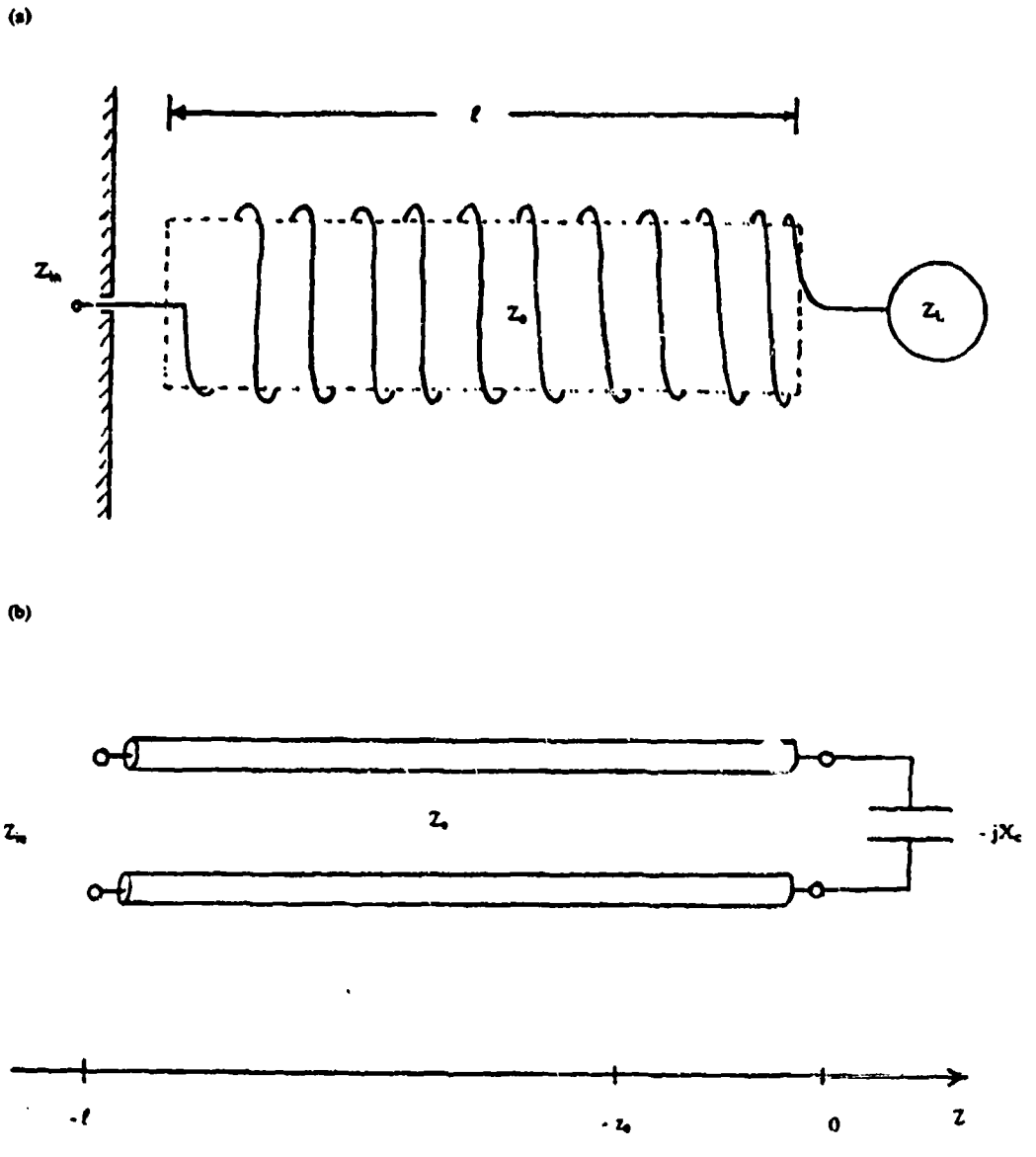

Figure 2. Helical resonator above a ground and the equivalent transmission line

Also, at the load end it is customary to define the complex load reflection coefficient Γ:

$$\Gamma_2 \triangleq \frac{V_-}{V_+} = \frac{Z_L - Z_0}{Z_L + Z_0} = |\Gamma_2| \angle\phi_2. \tag{40}$$

where Z_L is the impedance of the load and Z_0 is the effective impedance of the line. For a capacitive load, $Z_L = 1/(j\omega C)$, and for an open circuited line $\Gamma = 1 \angle \underline{0^\circ}$.

From Equation 39 we have, at the input end of the line,

$$V_{input} = V(-\ell) = V_+ e^{\gamma\ell} + V_- e^{-\gamma\ell} \tag{41}$$

where, again, Γ is a complex quantity defined at the load. Also from Equation 39, we may write the voltage at the load end as:

$$V_{Load} = V(0) = V_+ + V_- = V_+[1 + \Gamma] \tag{42}$$

Equations (41) and (42) may be combined in the following extremely useful expression which relates the load voltage to the input (generator end) voltage:

$$V_{top} = \frac{V_{base}[1 + \Gamma_2]}{[e^{\gamma\ell} + \Gamma_2 e^{-\gamma\ell}]} \tag{43}$$

This expression is probably the most important equation in all of high voltage RF engineering. It may be expanded for computational purposes as the expression

$$|V_{top}| = \frac{|V_{base}| \sqrt{[1 + |\Gamma_2| \cos\phi]^2 + [|\Gamma_2| \sin\phi]^2}}{\sqrt{[e^{\alpha\ell} \cos\theta + |\Gamma_2| e^{-\alpha\ell} \cos(\phi - \theta)]^2 + [e^{\alpha\ell} \sin\theta + e^{-\alpha\ell} |\Gamma_2| \sin(\phi - \theta)]^2}} \tag{44}$$

Now consider what happens on an open-circuited low-loss line one quarter wavelength long. Simple complex algebra gives the following well-known result:

$$V_{Load} = -j\left(\frac{V_{base}}{\alpha \ell}\right) \tag{45}$$

(for $\ell = n\lambda/4$ with n odd) where, again, α is the attenuation per unit length of the transmission line, and the j implies that the voltages at the two ends are in phase quadrature. The structure is a lossy, tuned reactive resonator. Since the numerator of this equation is finite and the denominator is vanishingly small, the voltage standing wave will build up to very large values. The transient growth process will evolve until either a system nonlinearity occurs or the line's I^2R losses are equal to the power being supplied by the source. The power driving the line, the line losses $\alpha\ell$, and the breakdown potential of the load geometry (which usually arises from the onset of cold field emission from the electrode) are what limits the maximum voltage ultimately attainable with this apparatus.

In order to carry out a numerical evaluation of this analysis, it is necessary to calculate the real and imaginary parts of the complex propagation constant and Schelkunoff's effective characteristic impedance for a helical resonator.[20] These can be found from the relations

$$\alpha\ell = \frac{R\ell}{2Z_0} = \frac{R_{loss}}{2Z_0} \tag{46}$$

$$\beta = 2\pi/\lambda_g \quad \text{where} \quad \lambda_g = V_f\lambda_0 \tag{47}$$

where the helix velocity factor, effective characteristic impedance, and attenuation are found from

$$V_f = v/c = \frac{1}{\sqrt{1 + 20(D/s)^{2.5}\,(D/\lambda_0)^{0.5}}}$$

λ_0 = free space wavelength
D = helix diameter
s = turn-to-turn spacing
(all in the same units) (48)

$$Z_0 = \frac{60}{V_f}\left[\ln\left(4H/D\right) - 1\right] \quad . \tag{49}$$

$$\alpha\ell = \frac{7.8125(H/D)^{1/5}}{d_w Z_0 \sqrt{f_{MHz}}} \text{ Nepers} \qquad (50)$$

where d_w = wire diameter in inches
H = height of helix = Ns
N = Number of turns

At this point, the engineering analysis is complete, and we are now ready to perform actual numerical predictions to compare with system measurements.

Summary of Operation

The secondary of a conventional resonance transformer is a helically distributed quarter-wave resonator, *not* a lumped tuned circuit - at least when it is operating in the regime where the primary has been open circuited. The voltage rise is by standing wave: $V_{max} \approx S\, V_{min}$, where S is the VSWR on the transmission line resonator. The actual measured voltage distribution on a transmission line resonator follows the first ninety degrees of a *spatial* sinusoid, much as it would on a quarter-wave vertical monopole antenna: V_{min} at the base and V_{max} at the top. In fact, resonance transformer engineering is exactly the same as designing top loaded vertical antennas. The only distinction is that a Tesla coil is *physically* short enough so that its radiation resistance is negligible. (In the absence of breakdown, very little energy is actually lost by radiation.)

These Tesla resonators perform equally well when driven by any high power *master oscillator* - spark gap, vacuum tube or solid state. (Efficiency and junction breakdown become major concerns with the latter two.) The theory and structures work at frequencies as high as several GHz (RF plasma torches). One structure that we employed in the lab operated at 145 Mhz. Figure 3 shows several such structures.

Comments

It is now clear why so many of the "Tesla Coils" used by early accelerator physicists (and even some today) performed so poorly[21 22 23] and why recent Russian Tesla transformers work so well. The early coils were usually constructed with thousands of turns (e.g., 7000 or more) of #36 gauge (or smaller!) copper wire, resulting in huge $e^{-\alpha\ell}$ propagation losses. For such machines, the SWR voltage rise is only a fraction of what is possible. The only way the early constructors could obtain high voltage from such poor designs was to overwhelm the losses by increasing the input power. [James Chadwick (the discoverer of the neutron), frustrated by his early failures to get Tesla resonators to work, recognized that something was wrong and said, "*I didn't have the proper conditions and training to carry out such things.*"[24]] From Equation 45, it is clear that very little power is actually required to attain extremely high voltages if $\alpha\ell$ is made small and good engineering practices are followed.

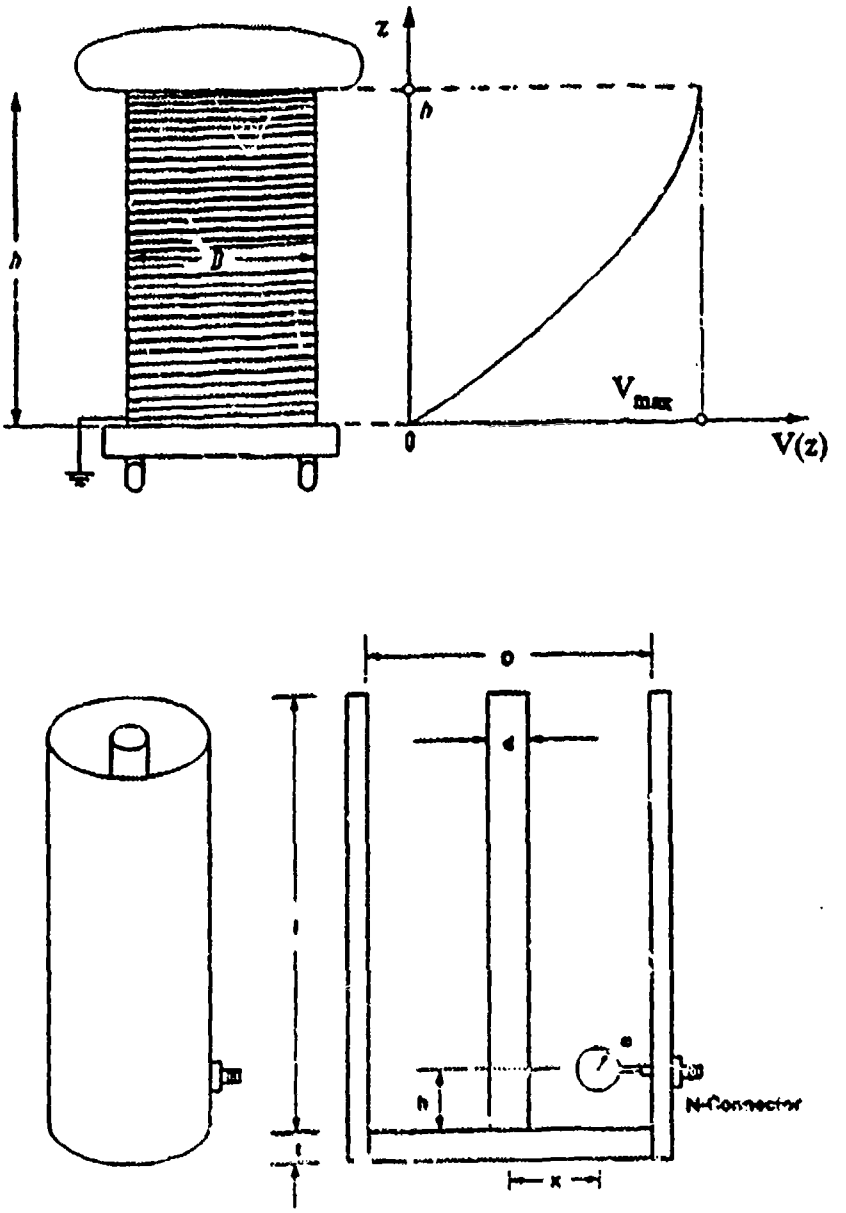

Figure 3. (a) Tesla resonator with voltage distribution. (b) VHF resonance transformer

Trapped Energy and Resonator Response Time

Although we employed a steady-state quasimonochromatic approximation for the analysis of the helix, we can address a basic question: How long does it take for trapped energy to cause a standing wave to form on a distributed resonator? (As stated above, we are not aware of any formal transient solution for a distributed lossy helix.)

Goldman has observed[25] that the build up transient time of a tuned transmission line must be inversely related to the selectivity, or spectral width, of the resonator, δf. This quantity is related to the resonator losses. Born and Wolf[26] and also Thomas[27] point out that the spectral width and the time duration of a wave train are not independent quantities, but satisfy a particular inequality called the "uncertainty relation." So, it should be apparent that the time taken for the waves to build up, from initial uniform energy storage (at the primary spark quenching instant), is inversely related to the spectral width of the resonator. This is the famous Fourier reciprocity relation:

$$\delta t \bullet \delta f \geq 1/(4\pi) \tag{51}$$

where δf is related to the resonator Q as $Q = f_o/\delta f$, and δt is a quantity often called the coherence time (for optical fields). We interpret the latter as the time duration required for coherent oscillations to build up on a distributed resonator and a standing wave interference pattern to form. We will discuss our laboratory measurements of this quantity in a later section. [In optics, temporal or self coherence (at a point in space) is the ability of a light beam to interfere with a time delayed sample of itself. The temporal "degree of coherence" is formally defined in terms of the autocorrelation function of the light, and it can be measured with an amplitude splitting Michelson interferometer. A finite duration "wave train" is the resultant disturbance produced by a Fourier sum of infinite duration spectral components. *Coherence time*, δt, is the effective duration of the wave train, and it is reciprocally related to the spectral bandwidth of the electromagnetic field.]

The laboratory measurement of these parameters and the interpretation of δt as the time to establish the high voltage VSWR pattern on resonance transformers will be discussed in the section on laboratory measurements below.

TESLA TECHNOLOGY LABORATORY MEASUREMENTS

Objectives

The purpose of this section is to examine the laboratory measurements associated with the RF portion of the equipment and compare these with the predictions of the analytical model. From these, we will be able to address the scalability issue.

Summary of Achievements

In this section we discuss the laboratory measurements and experimental verification of the analytical model advanced above. In particular, we were able to verify the effect of spark duration

and VSWR on performance. The electrical scalability issue was resolved. We were able to confirm the low frequency (145 Khz) and VHF (145 Mhz) behavior. Lastly, we were able to document the hypothesized resonator coherence time transient phenomenon.

Measured System Parameters

The measured lumped equivalent electrical parameters associated with Figure 1, used for much of the project, are given by

$L1 = 15\ \mu H$
$C1 = 0.16\ \mu F$
$R1 = 0.4$ Ohms
$M = 17.5\text{-}50\ \mu H$
$L2 = 0.015$ H
$C2 = 76$ pF
$R2 = 65$ Ohms
$Vo = 35$ kV
$C_T = 35$ pF
$t_s = 98\ \mu s$

Using these numerical values in the analytical expressions of the previous section give the predictions

$$k = \frac{M}{\sqrt{L_1 L_2}} = 0.037 - 0.24 \quad (0.072 \text{ typical}) \qquad (k_c = 0.014)$$

$$f_{oP} = \frac{1}{\sqrt{L_1 C_1}} = .03 \text{ kHz}$$

$$f_{oS} = \frac{1}{\sqrt{L_2 C_2}} = 149 \text{ kHz} \qquad (52)$$

$$f_1 = 149 \text{ kHz} \quad (\text{Eq } 25)$$

$$f_2 = 102.6 \text{ kHz} \quad (\text{Eq } 26)$$

$$V_{C2}(\text{peak}) = 213 \text{ kV} \quad (\text{at } t = 10\mu s)$$

$$V_{ind}(t_s) = 47.6 \text{ kV}$$

It should be noted that $V_{ind}(t)$ is not the same as the voltage appearing across C_2. That is, $V_{ind}(t) \neq V_{C2}(t)$. In the Kirchoff voltage law equation $i_2(t)$ is produced by $V_{ind}(t)$, and $V_{C2}(t)$ depends upon the integral of $i_2(t)$. We have plotted the measured and predicted $V_{C2}(t)$ waveforms in Figure 4. (There appears to be a small dc offset in the oscilloscope waveform. Such an artifact may have resulted from the HP 54510A digital sampling scope working in a laboratory environment with such intense electric fields.)

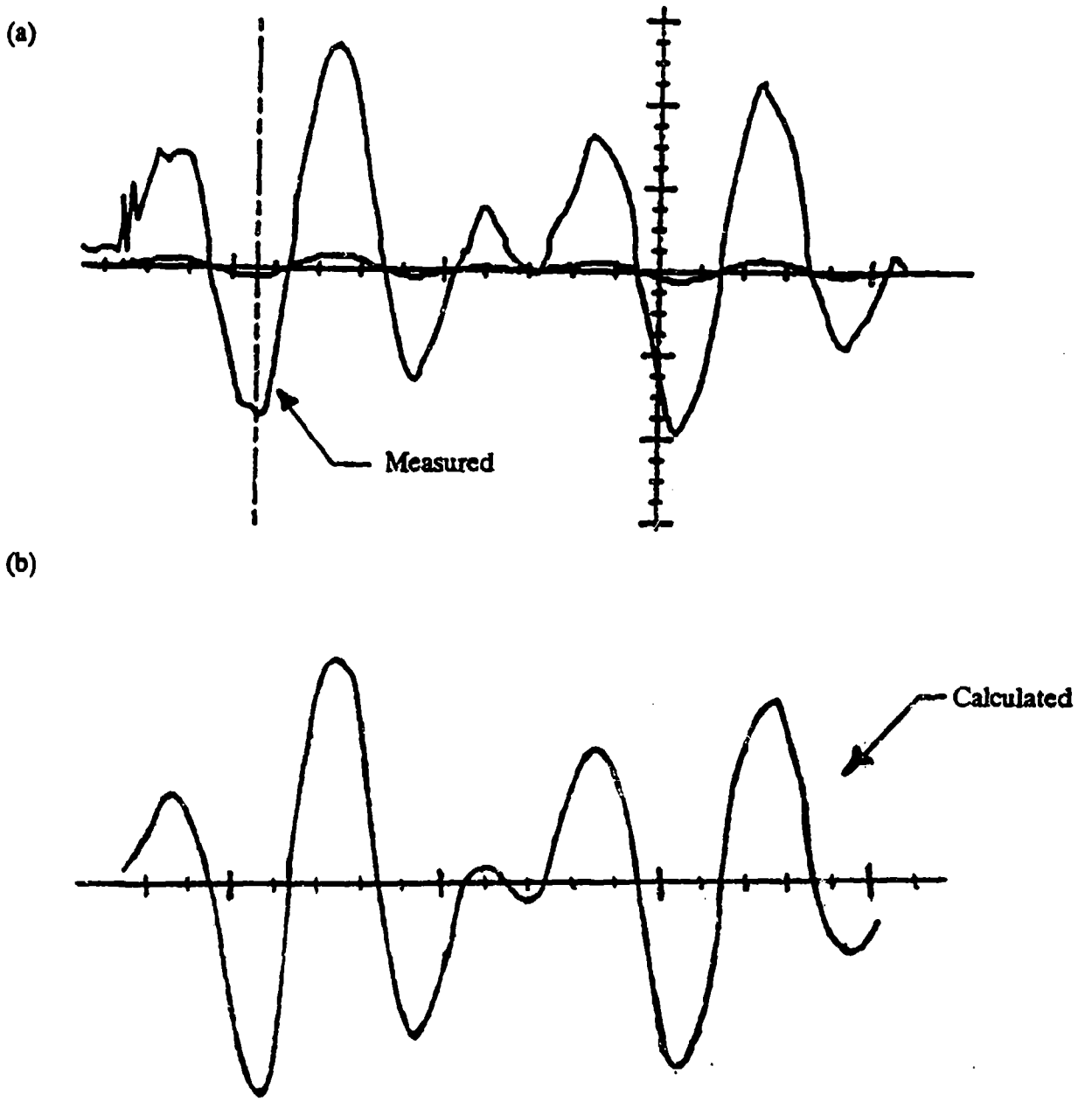

Figure 4. $V_{C2}(t)$: (a) Oscilloscope waveform. (b) Predicted by analysis

The $V_{C2}(t)$ waveform measured on the oscilloscope is shown *during* the dwell time of the primary spark ($t < t_s$). [It is desirable to have the primary spark break at the maxima of $V_{ind}(t)$, not $V_{C2}(t)$].

As an example of the usefulness of our analysis, we applied it to the resonance transformer stage. The helix was constructed with the following physical characteristics:

$D = 2.0$ ft
$S = 0.286$ inches between turns
$N = 342$ turns
$d_w = 0.102$ (#10 gauge silver plated copper)
$H = 97.8$ inches tall
$f_r = 143$ kHz (resonator worked against ground, with toroid in place).

The entire structure was painted with half a dozen coats of glyptol high voltage, moisture resistant sealer. The Q of the resonator was measured with a swept frequency source as $Q = 34.5$. The predicted transmission line parameters were

$Z_0 = 16{,}000\ \Omega$
$\theta = \beta\ell = 64.5°$
$R_{base} = 266\ \Omega$
$V_r = 0.0067$
$VSWR = 60$
$V_T/V_{base} = 54.3$
$V_T = 2.5$ MV.

While we had no instruments capable of measuring in the megavolt range, we could easily measure the ratio $V_T/V_{base} = 54$. Clearly, $V_T >> V_{C2,max}$. We readily obtained randomly directed electrical discharges in excess of 15 feet (and more if desired). There is a distinct advantage to operating in the distributed resonator mode as opposed to operating in the lumped element regime.

The physical behavior as a resonator is clearly seen when this information is plotted on a conventional Smith Chart. The toroid capacitance at 143 kHz produces a certain lumped-element load reactance, which must be normalized by the Z_0 of the helix. This is the normalized load impedance where the Smith Chart is entered. (See Figure 5.)

Moving $\phi = 2\beta\ell$ towards the generator places us exactly at the base of the resonator, showing that the slow wave helical structure is, indeed, in quarter wave resonance. Very large standing waves have been established. The latter do not occur in the lumped element regime for coils, where the voltage distribution is uniform over the entire inductor and the input impedance would be purely reactive ($j\omega L_2$, not R_{base}).

This leads us to a resolution of the scalability issue. There is a great deal of flexibility in the design equations presented above. We can keep the same output voltage and power, while shrinking the physical size of the structure by either shifting the operation from VLF (very low frequency) to VHF (very high frequency). Alternatively, we could even shrink the physical size of the structure and

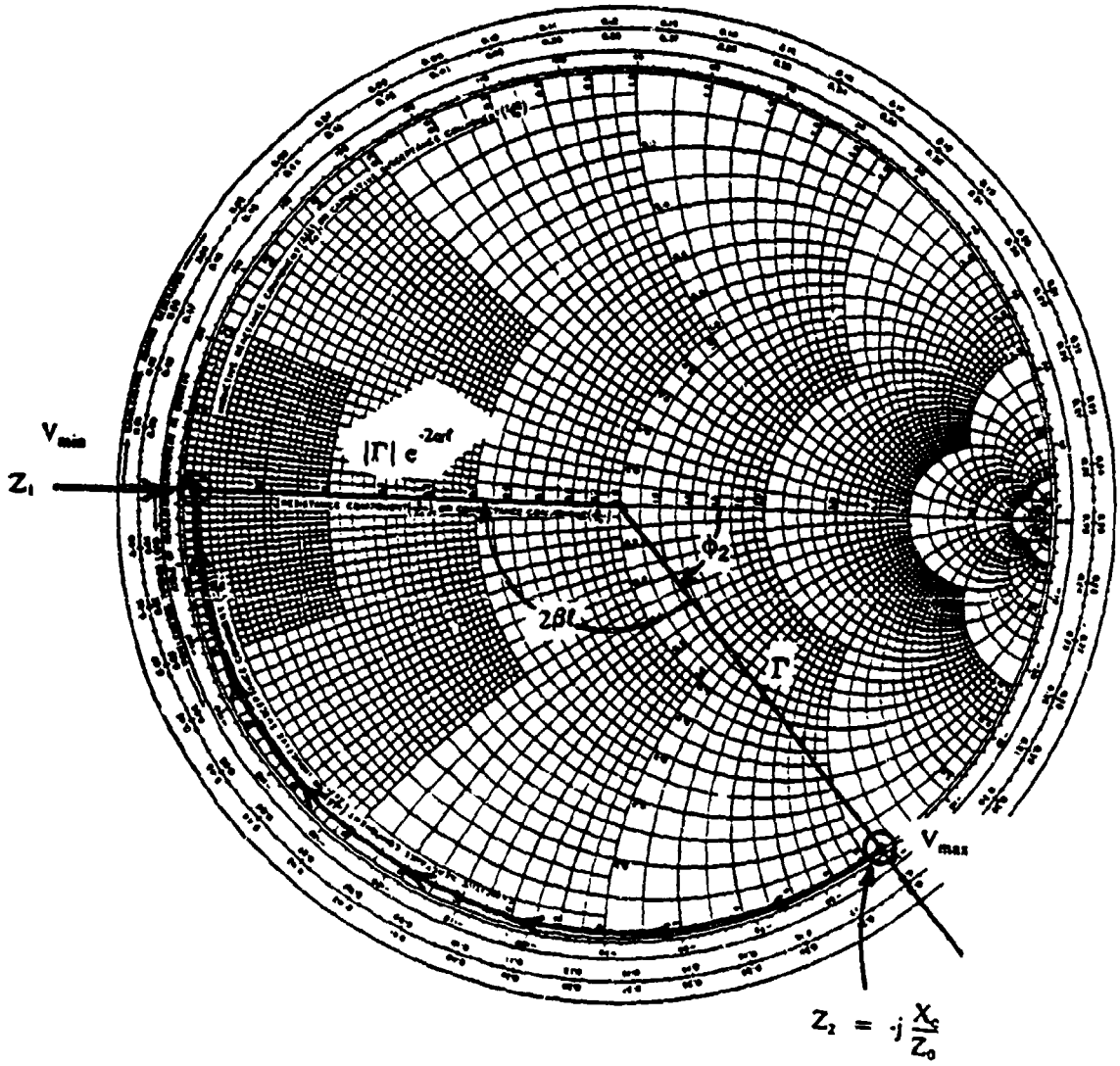

Figure 5. Smith chart presentation of our Tesla coil

remain at the same frequency simply by rewinding the helix so that its velocity factor, V_f (given above in the analysis), is reduced by the desired scale factor. When scaling these structures, the critical thing to watch is the propagation loss αt. (Don't scale down by going to a great number of turns of very fine wire!)

Coherence Measurements

While the primary break's spark is conducting, the system behaves as a lumped coupled oscillator, with energy interplaying back and forth between the primary and secondary and decaying down exponentially. If the primary can be broken at the appropriate time, the energy can be trapped in the secondary, where a standing wave interference pattern can be built up over a short time. We recorded the ***measured waveform*** shown in Figure 6, which specifically documents this phenomenon.

The "early time response" on the left shows the waveform ringing down while the primary spark is conducting. During this interval, the waveform exhibits beats, indicating that the system is behaving as lumped coupled coils. The primary spark is extinguished at the center of the graph, and there exists a "transition epoch" during which the voltage on the structure rises up to a maximum. The wave then proceeds to ring down monochromatically (indicating that the primary and secondary are no longer coupled). We have identified the transition epoch, during which the voltage wave builds up, as the "coherence time." We take δt as the time duration required for coherent oscillations to build up on a distributed resonator of $Q = f_0/\delta f$ and a standing wave interference pattern to form.

Because of the huge voltage rise that can be made to occur after the spark breaks it is difficult to present the data, but the figure does show what actually happens, even on a moderately lossy structure. The predicted coherence time, from the Fourier relation is

$$\delta t = 1/(4\pi\delta f) = Q/(4\pi f_0) = 19.2\ \mu s.$$

The figure shows the actual voltage build up at the top of the resonator, after the primary spark has been quenched. The build-up interval starts with the vertical marker shown at $t = 172.5\ \mu s$ and concludes with the marker shown at $t = 191.0\ \mu s$. The transient build-up time interval is 18.5 μs. By the way, the time interval between peaks of the waveform during the "late time response" is also displayed as 7 μs, corresponding to a resonator ring-down frequency of 142.857 kHz.

The measured coherence time was in excellent agreement with the predicted value (less than 5% difference). This experiment was subsequently repeated under less lossy conditions, and we were able to not only document the coherence time build-up, but also to demonstrate that the voltage at the top of the resonator was able to exceed the lumped mode V_{C2} value by a factor of 43. We take it that, within the range of experimental error, the concept of resonator coherence time is quite meaningful, and the physics of resonator mode standing wave build-up is now experimentally established. These new experimental results clearly demonstrate that one can readily surpass the so called "$k = 3/5$ optimum coupled system" determined by Finkelstein for lumped circuits.[28] We invite other investigators using pulsed resonance transformer technology to explore this newly documented phenomenon.

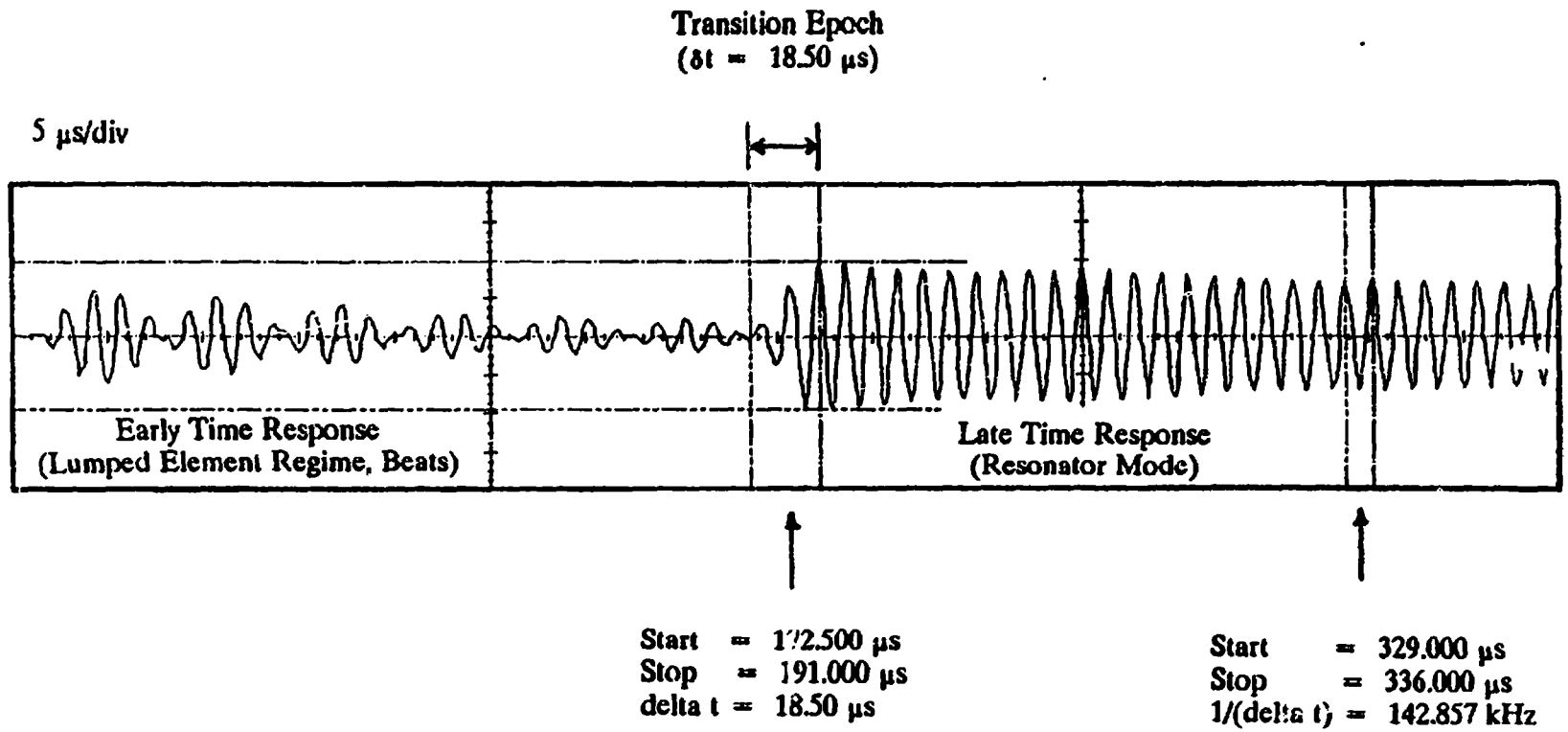

Figure 6. Measured resonator transient waveform. Note that the primary spark conducts during the early time response.

Construction Comments

Our laboratory experience has led us to the following practical construction suggestions, which have not yet appeared in the professional literature. They are in stark contrast to the previously accepted optimum design criteria suggested by Finkelstein, et. al. in the classic reference just cited. If one follows these new suggestions, one will find that the resonance transformer will operate in the transmission line regime, and its output will far surpass that of the previously so called "optimum" machine.

1. Construct the resonator to have the lowest propagation losses possible. (Use the heaviest gauge conductor on the lowest loss form possible.)

2. Use the tightest coupling possible. (Make $k > > 0.6$ if possible without primary-secondary arc-over.)

3. Adjust the primary spark duration to match "the optimum spark duration," t_s.

If one does not have the technology available to perform item 3, there is an alternative procedure that can be followed:

3'. Employ a small low loss coil, called a regulating coil, in series with the primary and adjust it to compensate for t_s.

The regulating coil is a series primary inductance with no magnetic coupling to the secondary. This will permit one to adjust the apparatus until its optimum t_s has been lengthened to match the switching duration of the given machine. It is desirable to make the mutual inductance, M, large (within practical geometrical limitations), while at the same time making the component of the primary inductance which is magnetically coupled to the resonator small (but not so small that the regulating inductance can't be adjusted to compensate for it). Following these steps will quickly lead to the desired operation.

Final Remarks

The most significant feature of the resonator mode operation is that it provides a physical insight not possible with the lumped circuit approach, which totally fails to describe the distributed resonator mode of the resonance transformer. What limits the maximum voltage attainable for a given system? The power spectrum driving the structure, $1/\alpha t$ and the breakdown potential of the top electrode are the only limitations. If we have a large enough electrode with no shunt losses, and can reduce helix losses - there is no fundamental limit in classical physics on the voltage rise. It is now clear that the RF apparatus operates linearly and can be scaled to match the requirements of the specific application.

ELECTRICAL DISCHARGES AND LABORATORY TESTING

Experimentation

Our experiments included the construction of a vacuum tube having a single electrode aluminum cathode. We employed a variety of fabrication techniques and construction materials. The first tube was pumped down and excited from the top terminal of the resonance transformer. Its initial operation was promising: three inch diameter visible glow surrounded the linear portion of the megavolt discharges near the tube. (This may have been bremsstrahlung radiation or it may have been due to intense corona.) The tube permitted directed discharges out to a distance of 2 - 4 feet, at which distance the discharges again forked and behaved as usual, spraying in a more-or-less "lightning-like" manner out another 5 feet. After a brief operation (about 1/2 minute), the terminal voltage was increased several hundred kV more, and the face plate of the tube emitted a 1/2 inch diameter fireball and the forking of the discharges out in the air backed up to the front of the tube. The "fuzzy blue glow" which had surrounded the directed discharge channel (like a thick sleeve of blue mist) "evaporated," and the discharge was no longer directional, but forked and sprayed upward from the diode structure itself. (We had been able to "shoot" the discharge downward at a depression angle of 45°. This is usually impossible, since the hot discharges will rise and dart upward.) Upon inspection, the face of the tube had an elliptical puncture 1/32"x3/32," and the inside of the tube was covered with carbon soot.

Channel Seeding, Ball Lightning, and Directed Discharges

During our experimental research, we spent some time on Teflon vacuum tubes and we experienced rather astonishing results with the initial tests. At that time we observed a directed discharge on the order of four feet. This is to be distinguished from the more or less undirected electrical discharges ("RF lightning") from the top of the Tesla resonator, which can easily reach 10-20 feet in random directions in the space available in the laboratory.

As part of the project, we were contracted to examine the effects of channel seeding mechanisms and materials. It is now clear to us that the early straight line discharge, which we experienced probably followed *a directed jet of carbon macrons* issuing from a puncture in the fore wall of the tube. This holds some degree of similarity to our recent discovery of an RF initiated ball lightning mechanism.

The concept of macron-directed discharges can be grasped from a consideration of photographs published of our ball lightning research. Photograph 1 is rather dramatic.

It was presented at several symposia and published in our 1990 article in Soviet Physics Uspekhi.[29] It shows more than a dozen large spherical fiery globules all in a row, being struck by and directing the propagation of a large streamer. The film was ASA 400 and the shutter speed was 1/4 second. Lifetimes up to several seconds could be documented by means of video recording. There is a 30 cm diameter high voltage electrode which can be seen off to the left. In those publications, we were fairly successful in describing the physics in terms of fractal phenomena.

Photograph 1. A spray of fire balls emanating from a high voltage terminal, directing a discharge. From Corum and Corum, 1990.

Combining the ball lightning work with the present observations of directed energy leads to some startling conclusions. It should be noted that merely shooting out a wire from a high voltage electrode to a target will not really direct a discharge. Maxwell's equations require that the tangential component of the electric field vanish in a perfect conductor. As a result, the electric field around a wire must be purely radial. (It must be normal to the wire.) If the fields are intense, as in our case, the radial electric fields will incite a radial avalanche discharge around the wire, and the energy will bleed off in a cylinder of corona discharge. (See Photograph 2.)

However, if the conducting path is broken up into a particulated stream of micro sized conducting macrons (say, for example, in the 10-100 micron regime) the electric field possesses a substantial longitudinal component, with very little radial component. The situation is shown in Figure 7.

Two advantages are immediately apparent. First, the discharge is directable with very little radial loss. Second, the charged macrons possess an electrically reduced drag, which should be of significance in the hypervelocity regime. We understand the conventional wisdom concerning traditional mechanical hypervelocity macrons - that they, like micrometeorites, will loose their momentum over very short propagation trajectories (e.g. a few meters, more or less). However, we believe that, for *electrically charged macrons*, this traditional conclusion, apparently based on Whipple's famous analysis,[30] is erroneous. The classical mechanical drag theory for *uncharged* microscopic particles does not explain the significantly reduced drag on highly charged macrons (near the field emission limit). This important consideration, evidently, has gone unrecognized by researchers in the ballistics community (where q/m is negligible), and is of little consequence in the accelerator community (where q/m is huge).

The first advantage has also recently been discovered independently by other investigators. It appears in a technical publication on sequential plasma focusing.[31] In that paper, it is hypothesized that downstream floating conductors become auxiliary anodes, producing a cascade of secondary focusing events. The author was able to direct plasma discharges, in this manner, to a distance of several feet in an enclosed plasma chamber.

During our research, however, we had been able to direct the beam with copper dust macrons over distances of more than 27 feet in open air, and we have no doubts that ranges of two or three times this are readily obtainable - even with smaller equipment than we are presently using.

Photograph 3 shows the random discharges from an undirected discharge in (a), and from a directed discharge in (b). It is our opinion that this type of charged macron directed beam is much more **stable** and can convey much larger currents than conventional electron beams. It provides a longitudinal field which may, in fact, be employed to accelerate charges in air or vacuum. [We also believe that it is possible to initiate the macron beam with high voltage RF and then launch an intense low frequency (or even dc) current from the RF low impedance point up through the resonance transformer and out along the directed beam. This would provide a directed weapon with controlled lethality.] We therefore suggest that a hypervelocity stream of macrons can be used to bore a low density channel through the atmosphere to direct a relativistic electron beam which will "follow" the low impedance path created by the hypervelocity macrons.

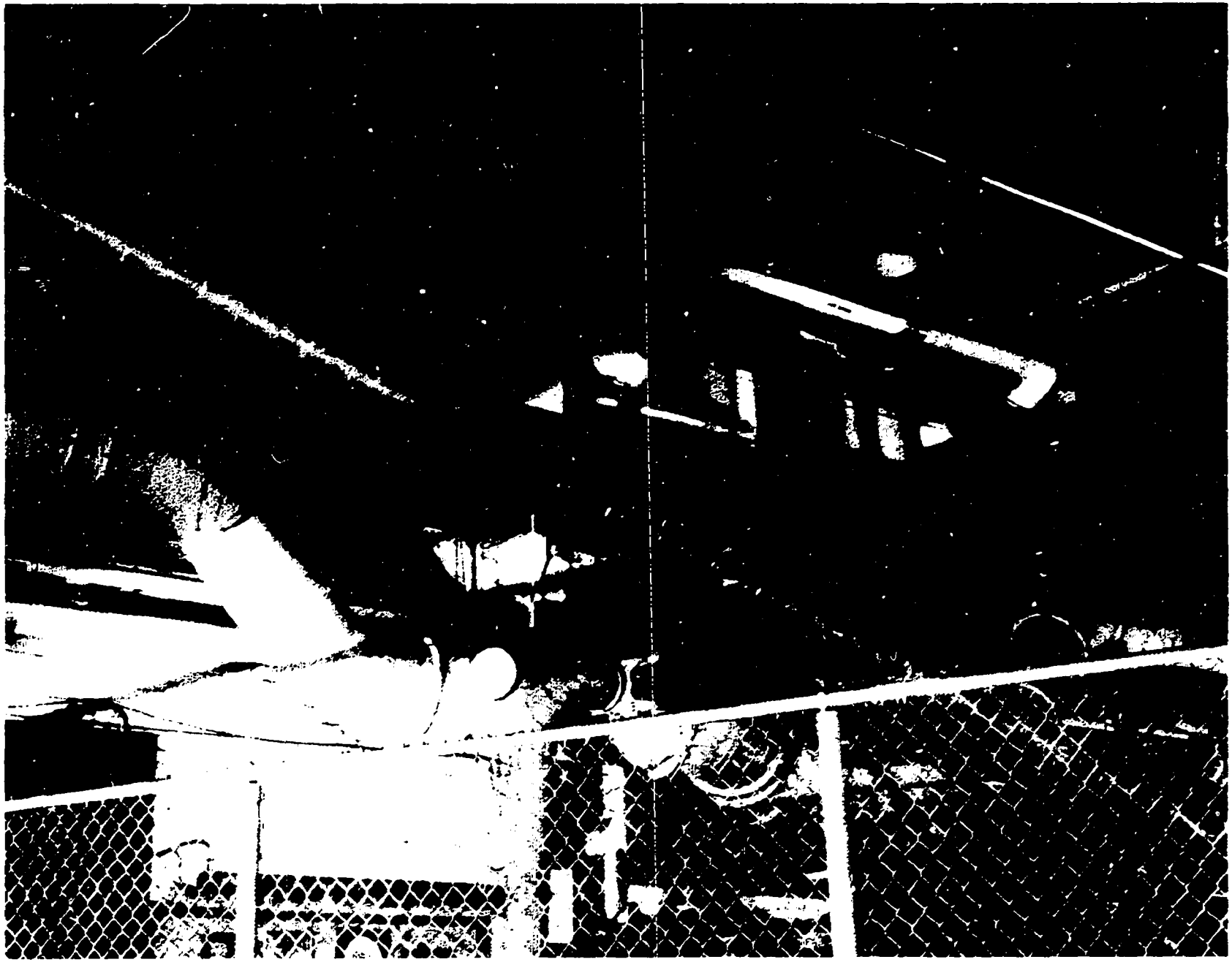

Photograph 2. Corona surrounding a conducting wire.

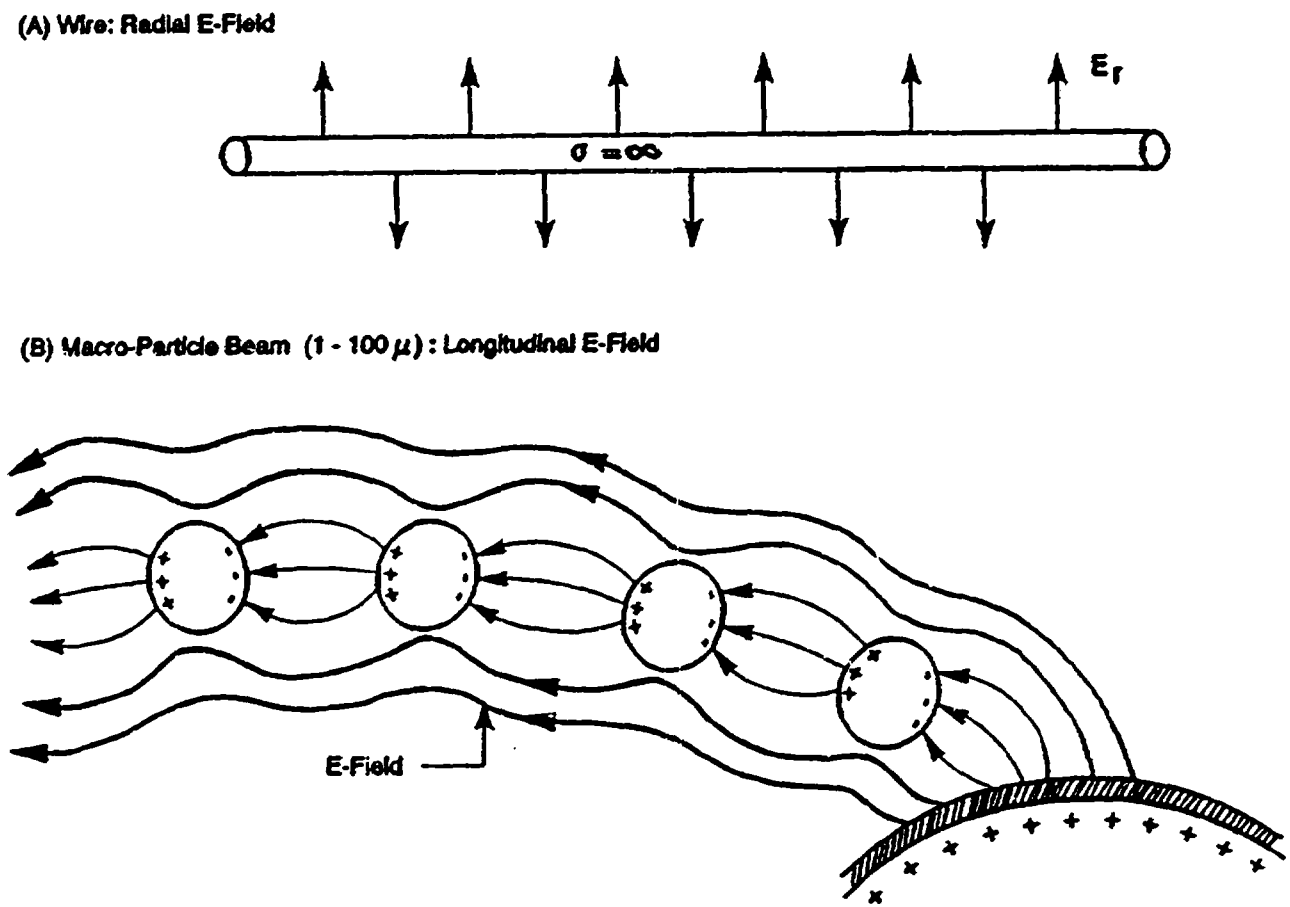

Figure 7. Electric fields produced by (a) a charged wire, and (b) a macro-particle beam

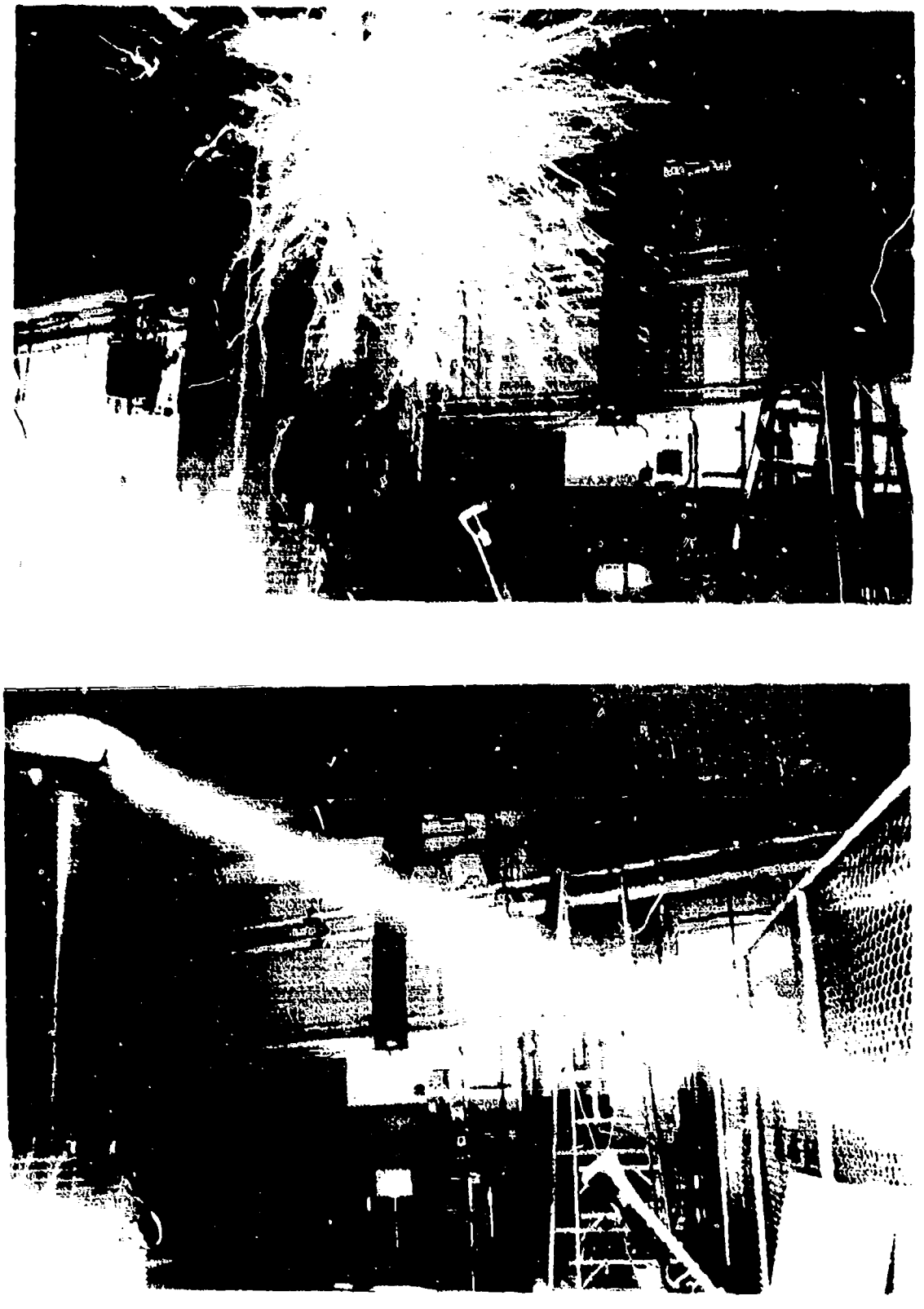

Photograph 3. Electrical discharges emanating from a high voltage terminal. (a) random discharge. (b) Seeded channel directed discharge.

Holeboring by electrically charged (reduced drag) macrons can also be modeled using Winterberg's analysis of holeboring[32] discussed earlier. When a charged high speed macron encounters ambient air the macron will heat the surrounding air and loose kinetic energy in the process. Another macron following in the previous particle's wake encounters a reduced density channel, and the drag forces on the follow-on particle are further reduced. Let e_o represent the distance over which a particle has heated the ambient air to an average temperature T from an ambient temperature T_o. The heated channel now has a lower density ρ than the ambient density ρ_o. If a stream of n particles takes advantage of this reduction in air density to penetrate further into the atmosphere the total penetration length e_n is found to be

$$e_n = \{1 - (1 - x)^n\}e_o/x \tag{53}$$

where $x = T_o/T = \rho/\rho_o$.

The macron particles then have two purposes. They provide a low density channel through the atmosphere for the beam which greatly reduces beam energy losses and scattering (Nordsieck expansion), and the particles provide a sequential self focusing mechanism which will keep the beam in the channel and possibly damp out beam instabilities. This discovery should be investigated further.

CONCLUSIONS

The Tesla transformer investigated in this project represents a viable high average power alternative to the conventional high-peak/low-average power processing employed in much particle beam research. The increased high voltage operating mode is particularly appealing. It appears that the maximum voltage attainable is limited only by insulation breakdown and the geometry of the structure.

With the successful attainment of an open air REB weapon, the fragility of the vacuum diode will have to be overcome, and a rugged alternative for future vacuum tubes must be investigated. We have discussed an experimental alternative to elementary particle beams in this research.

We believe that a combined macron/REB technique is the only near term practical solution for weaponizable fundamental charged particle beam devices in open air. (Sequential beam focusing then becomes possible.) We have expressed our belief that charged macron beams (beams of electrically charged particles with diameters in the 10 - 100 micron range) are considerably more stable and will convey much larger currents in air than relativistic electron beams alone. We think that the discovery of this channel seeding mechanism, and its impact on conventional particle beams, should be followed up at once.

REFERENCES

1. "A Radio frequency High-Voltage Generator," by David H. Sloan, Physical Review, Vol. 47, No. 1, January 1, 1935, pp. 62-71.

2. Lawrence and His Laboratory, by J.L. Heilbron and R.W. Seidel, University of California Press, 1989, pp. 116-121.

3. "On the Road to Tomsk," by M. Kristiansen, A. Gunther, and J. Thompson, Physics Today, June 1990, pp. 36-42. (See Table, pg. 41.)

4. Industrial Electron Accelerators, by E.A. Abramyan, Hemisphere Publishing Corp., 1988, 86-89, 93-102, 129-131.

5. Static and Dynamic Electricity, by W.R. Smythe, McGraw-Hill,Second Edition, 1950, PP. 340-347. Note the error in Section 9.12, Equation 14, where C1,2 should read C2,2.

6. "A Technical Analysis of the Extra Coil As A Slow Wave Helical Resonator," by J.F. Corum and Kenneth L. Corum, Proceedings of the 2nd International Tesla Symposium, Colorado Springs, Colorado, 1986.

7. Corum, J.F., Edwards, D.J., and Corum, K.L., **TCTUTOR - A Personal Computer Analysis of Spark Gap Tesla Coils**, Published by Corum & Associates, Inc., 1988, [110 page text + Disk, ISBN 0-924758-01-5].

8. "New Principles of High Power Switching with Semiconductor Devices," by I. Grekhov, Solid-State Electronics, Vol. 32, No. 11, 1989, 923-930.

9. Novye Printsipy Kommutatsii Bol'shikh Moshchnostei Poluprovodnikovymi Priborami (New Principles for Switching High Power Using Semiconductor Devices), by V.M. Tuchkevich and I.V. Grekhov, Leningrad, Nauka Press, 1988.

10. "Ultrahigh Voltage Silicon P-N Junctions with a Breakdown Voltage above 20 kV," by E.V. Astrova, et. al., Solid-State Electronics, Vol. 32, No. 11, 1989, pp. 851-852.

11. Electronic and Radio Engineering, by F.E. Terman, McGraw-Hill, 4th edition, 1955, Pg. 58.

12. "The Application of Low-Frequency Circuit Analysis to the Problem of Distributed Coupling in Ultra-High-Frequency Circuits," by R.W.P. King, Proc. I.R.E., November 1939, pp. 715-724.

13. "General Amplitude Relations for Transmission Lines with Unrestricted Line Parameters, Terminal Impedances, and Driving Point," by R.W.P. King, Proc. I.R.E., December 1941, pp. 640-648.

14. Fields and Waves in Communication Electronics, by S. Ramo, J.R. Whinnery and T. Van Duzer, Wiley, 1984, pg. 209. (See Problem #4.10b.)

15. "Transient Scattering from Bodies Designed with Loads or Layers," by T.L. Larry and M. Van Blaricum, Proceedings of the First Los Alamos Ultra Wideband Radar Symposium, March 7, 1990.

16. "A Technical Analysis of the Extra Coil As A Slow Wave Helical Resonator," by J.F. Corum and Kenneth L. Corum, Proceedings of the 2nd International Tesla Symposium, Colorado Springs, Colorado, 1986.

17. "The Application of Transmission Line Resonators to High Voltage RF Power Processing: History, Analysis, and Experiment," by J.F. Corum and K.L. Corum, Proceedings of the 19th Southeastern Symposium on System Theory, Clemson University, Clemson, South Carolina, March 1987, pp. 45-49.

18. "Tesla Coils: 1890-1990 - 100 Years Of Cavity Resonator Development," by J.F. Corum and K.L. Corum, Proceedings of the Fourth International Tesla Symposium, Colorado Springs, Colorado, July 1990.

19. Vacuum Tube Tesla Coils - Published by CPG Communications, Inc., 1988, (160 pages). [ISBN 0-924758-00-7].

20. "The Application of Transmission Line Resonators To High Voltage RF Power Processing: History, Analysis and Experiment," by J.F. Corum and K.L. Corum, Proceedings of the 19th Southeastern Symposium on System Theory, Clemson University, 1987, pp. 45-49.

21. "A Laboratory Method for Producing High Potentials," by G. Breit, M.A. Tuve and O. Dahl, Physical Review, Vol. 35, January 1930, pp. 51-65.

22. "The Application of High Potentials to Vacuum-Tubes," by M.A. Tuve, G. Breit and L.R. Hafstad, Physical Review, Vol. 35, January 1930, pp. 66-71.

23. "A Combined Tesla Coil and Vacuum Tube," by C.C. Lauritsen and R. Crane, Reviews of Scientific Instruments, Vol. 4, No. 9, September 1933, pp. 497-500.

24. "History of the Invention and Development of Accelerators," by A.F. Grinberg, Soviet Physics - Uspekhi, Vol. 18, No. 10, 1976, pp. 815-831. (Usp. Fiz. Nauk, 117, October, 1975, pp. 333-362.)

25. Frequency Analysis, Modulation and Noise, by S. Goldman, McGraw-Hill, 1948, PP. 134-139.

26. Principles of Optics, by M. Born and E. Wolf, Pergammon Press, 5th edition, 1975, PP. 316-320, 499-502, 505-506, 540-544.

27. An Introduction to Statistical Communication Theory, by J.B. Thomas, Wiley, 1969, PP. 386-393.

28. Finkelstein, D., Goldberg, P., and Shuchatowitz, J., "High Voltage Impulse System," Review of Scientific Instruments, Vol. 37, No. 2, February 1966, pp. 159-162.

29 Corum, K.L. and Corum, J.F., "ЭКСПЕРИМЕНТЫ ПО СОЗДАНИЮ ШАРОВОЙ МОЛНИИ ПРИ ПОМС ВЫСОКОЧАСТОТНОГО РАЗРЯДА И ЭЛЕКТРОХИМИЧЕСКИЕ ФРАКТАЛЬНЫЕ КЛАСТЕРЫ" [High Vc RF Ball Lightning Experiments and Electro-Chemical Fractal Clusters]," Soviet Physics - Uspekhi, Vol. 160, No.4, April 1990, pp. 47-58. (In Russian; See photograph 8, pg. 56.)

30. Whipple, F., "Meteors and the Earth's Upper Atmosphere," Reviews of Modern Physics, Vol. 15, 1943, pp. 246-264.

31. Lee, S., "A Sequential Plasma Focus," IEEE Transactions on Plasma Science, Vol. 19, October 1991, pp. 912-919.

32. Winterberg, F., "The Potential of Electric Cloud Modification by Intense Relativistic Electron Beams," Zeitschrift fur Meterologie, Vol. 25, pp. 180-191, 1975.

APPENDIX

COLLATERAL TECHNICAL ISSUES AND TECHNOLOGIES

The following items are collateral to the major topics of our research. If such a project as ours develops into a desirable effort, then each of the items below will need to be investigated.

HV Switching

The rotary break switching technology which we are employing is from the early world war II days - and that evolved from the early days in "wireless" around the turn of the century. (See the MIT Radiation Lab Series, Vol. 5 - Pulse Generators, by Glascoe and Lebacqz.) Unfortunately, not much has been done to improve high voltage RF switching technology since then. A great deal of effort has been expended on high power switches (for rail guns, EMP simulation, Marx generators, Laser triggering, etc.) but, to the best of our knowledge, none of the devices developed are useful for the type of high voltage RF power conditioning which we were doing. Mechanical rotary breaks need to be improved upon, or an alternative technology needs to be found.

The set of specifications for a new RF switching technology would be as follows:

1. Switch voltage: 100,000 (open), 0 (closed)
2. Switch current: 10,000 amperes at RF (not dc)
2. Switch impedance (at 1MHz): ∞ (open), 0 (closed)
3. Switching speed: from DC to at least 500 kHz
4. Pulse duration: 1 μs to 300 μs (variable control)

The most critical parameter here is the switch duration while the primary capacitor RF current is flowing. One desires to get this down on the order of 10 microseconds. Three hundred, even 100, microseconds is far too long for efficient HV operation. The problem is a lot like controlling the spark dwell (switch "on" duration) and engine RPM (# of pulses per second) on an automobile, only doing it with RF.

HV Insulation Materials

These will have to be conformable to our particular application. If better HV RF insulating materials can be found, then the apparatus size and weight can be greatly reduced (e.g., a factor of 5 or 10 would not seem unreasonable).

HV Rectification Process

Although our resonant transformer project feeds HV RF to the load, we can see where it could be very important to convert the high voltage RF to DC. That is, where 5 MV DC at 100 kW average power would be employed. (The power requirement precludes the use of traditional "electrostatic" machines, Marx generators, etc.) We think that RF physics exists to meet such requirements, but research and development would be required.

Meteor Directed Lightning

Although resonance transformers were the object of this research, we can envision several applications of this technology which can be employed to help beams propagate to greater distances, and overcome instabilities. For example one might employ hypervelocity "meteorites" to provide hole boring mechanisms for charged particle beams to follow in the atmosphere. This technique is a natural one for the HV RF power processing apparatus which was employed in this program. [We think that this may prove as a successful route to follow for a directed beam weapon. The effects promise to be several orders of magnitude beyond that possible with an REB alone, and the stand-off range may attain the several kilometer goal.]

Recycled Light, Power Multiplication, and Power Compacting

There is a technique presently being proposed for the new national laser gravitational radiation observatory, which will increase the laser power by a factor of 1000. The technique is called "recycled light" and is a laser version of an RF technique invented forty years ago by F.J. Tischer. The microwave version (appropriate for use with Tesla coils) is called "ring power multiplication."

At microwave frequencies, RF power is injected into a full wavelength ring resonator through a directional coupler. The RF in the ring resonator propagates in one direction with the correct phase so that power from the source continues to pump up the real power in the ring. Power multiplication by several orders of magnitude was observed back in the early 1960's, but SDI or HPM and UWB weapons were unforeseen at that time. We think that this technique could be used in conjunction with the resonance transformer technology which was employed in this project. This would be an area for future research and applications.

Along the same lines, we can also mention a technique called "power compacting." Simply stated, the idea is to pump RF power into a standing wave resonator (like a length of wave guide, or even a Tesla coil) and then quickly move the short circuit end in, spatially compressing the RF energy, and raising the energy density. The compressed RF energy can then be released in a shorter time with a higher peak power.